Study of the starch grains of tubers using Mueller matrix microscopy

Author: Aleix Ramon Bobi Olmo
*Facultat de Física, Universitat de Barcelona, Diagonal 645, 08028 Barcelona, Spain.**

Advisor: Oriol Arteaga Barriel

Abstract: In this TFG the subject of study are starch granules from potatoes and sweet potatoes. The characterization of both tubers is made by several measurements of their Mueller matrix using the Mueller matrix microscopy technique. Then the birefringence has been calculated from these measurements in order to determine the microscopic structure of the starch granules.

I. INTRODUCTION

In the study of light transmission through materials and the effect of those materials properties on the polarization of light, we use the Stokes-Mueller formalism, based on intensities, to describe them due to the fast temporal variation of the electromagnetic fields we are working with. Mueller matrices describe the transformation of the Stokes vector for some sort of light source which has been previously polarized in some direction and that has certain properties such as degree of polarization or the retardation angle between orthogonal axes. The Stokes vector is described as:

$$\mathbf{S} = \begin{pmatrix} I \\ M \\ C \\ S \end{pmatrix} = \begin{pmatrix} I_T = I_X + I_Y \\ I_X - I_Y \\ I_{45} - I_{-45} \\ I_R - I_L \end{pmatrix} \tag{1}$$

where the subscripts indicate the direction of polarization: linear horizontal (X), linear vertical (Y), linear at 45°, linear at −45°, left circular (L) and right circular (R). The Mueller matrix (MM), $\mathbf{M}$, is described as:

$$\mathbf{M} = \begin{pmatrix} m_{11} & m_{12} & m_{13} & m_{14} \\ m_{21} & m_{22} & m_{23} & m_{24} \\ m_{31} & m_{32} & m_{33} & m_{34} \\ m_{41} & m_{42} & m_{43} & m_{44} \end{pmatrix} \tag{2}$$

The MM does the transformation of an incoming Stokes vector in a outcoming vector $\mathbf{S}_{out} = \mathbf{M}\mathbf{S}_{in}$.

Mueller matrix measurements are applied in different fields, such as material science, biology, astronomy, biomedical etc. The Mueller matrix microscopy technique does MM measurements with high spatial resolution which is often achieved by using microscope of objectives and cameras as a detectors. One interesting use for Mueller matrix microscopy is the study of the birefringence, especially in vegetable crops such as Ramie [1]. This will be one of the main objectives of this TFG, specifically focused on the study of birefringence for starch grains of potatoes and sweet potatoes, while also looking for other proprieties and exploring the resolution of our Mueller matrix microscope. All these measures will be taken imaging with a camera, which is one of the two main approaches that are used in the study of MM with spatial resolution (the other method is based on a mapping approach with a single point detector). The camera used in the measures can detect light from the near IR to the visible spectrum. For the measurements reported in this work, we used a central wavelength around 535 nm corresponding to green light.

Birefringence is the main optical property that will be studied in this work. Birefringence is the property of an anisotropic material having two different refractive indexes for two orthogonal polarizations, usually known as ordinary (n_o) and extraordinary (n_e). The retardation is related to the difference of refractive indices as:

$$\delta = \frac{2\pi(n_e - n_o)d}{\lambda} \tag{3}$$

The difference between the refractive ($n_e - n_o$) indexes can be measured if one knows the thickness of the material (d) and the wavelength (λ).

II. MEASUREMENT METHOD

The measurement equipment is composed of a light source, a polariser, a compensator that rotates to 7 different angles, the sample, the objective and the camera. The Stokes vector reaching the camera can be determined using:

$$\mathbf{S_{out}} = \mathbf{M_S}\mathbf{M_c}(\theta)\mathbf{M_P}\mathbf{S_{in}} \tag{4}$$

where $\mathbf{M_P}$ is MM of a linear polarizer, $\mathbf{M}_c(\theta)$ is the MM of a rotating compensator and $\mathbf{M_S}$ is the MM of the sample. The measurements have been done imaging with a polarization camera. This type of camera has a sensor based on 4 sub-pixels grouped together forming one super pixel. Each one of these sub-pixels measures one of the four types of linear polarized light (X, Y, 45°, −45°) that we need for detecting the 3 first Stokes components, as it is shown in FIG. 1.

For the first part of the set-up, light beam travels through the linear polariser and the compensator,

*Electronic address: abobiolm57@alumnes.ub.edu

FIG. 1: Representation of the disposition in which are assigned each pixel in the super pixel. [2].

which can rotate, so the Mueller matrix for this part is known: $\mathbf{M}(\theta) = \mathbf{M_c}(\theta)\mathbf{M_P}$. The Stokes vector reaching the sample will be also known (natural light can be used as input Stokes vector) and it may be written as $\mathbf{S}(\theta)^T = (S_1, S_2, S_3, S_4)$. When it passes through the sample it results in $\mathbf{S'}$ where $\mathbf{S'} = \mathbf{M_s}\mathbf{S}(\theta)$, leading to the following equations:

$$m_{11}S_0 + m_{12}S_1 + m_{13}S_2 + m_{14}S_3 = S'_0 \quad (5)$$

$$m_{21}S_0 + m_{22}S_1 + m_{23}S_2 + m_{24}S_3 = S'_1 \quad (6)$$

$$m_{31}S_0 + m_{32}S_1 + m_{33}S_2 + m_{34}S_3 = S'_2 \quad (7)$$

$$m_{41}S_0 + m_{42}S_1 + m_{43}S_2 + m_{44}S_3 = S'_3 \quad (8)$$

The camera can detect S'_0, S'_1, S'_2, but not S'_3, which means that the last row of the MM (elements m_{41}, m_{42}, m_{43}, m_{44}) cannot be measured. The fourth row can be calculated assuming that there is no depolarization of the light while travelling through the sample. The degree of polarization is defined as:

$$DOP = \frac{\sqrt{S_1^2 + S_2^2 + S_3^2}}{S_0} \quad (9)$$

Even though the camera cannot measure circular polarization (S_3), assuming that the sample does not depolarise (DOP=1), it is possible to determine S_3 as $S_3 = \sqrt{S_0^2 - S_1^2 - S_2^2}$. This equation has two solutions with opposite signs. A method was published to determine the correct sign by combining data coming from several diferent angles and it is discussed in [3].

The samples were prepared by rubbing a slice of potato or sweet potato on a microscope slide. The slides were then analysed with the microscope and the MM measurement were made in the areas where starch grains were observed. One problem that I had in the first two measurements was that there were "black areas" surrounding the starch granules which made impossible the full analysis of the granules. This phenomenon was caused by the deviation of the light in the outer surface of the granules due to their spherical shape, producing a non-normal incidence on the angle of the incident light. The big difference between refractive indices of air and starch produced a deviation of the light beam by reflection and refraction effects at the interfaces. This problem was solved in the following measurements by a drop of oil between the microscope slide and the cover slip. Oil has a similar n to the granules so the interface effects are minimized and the rays could travel straight through the granules and be received by the camera. FIG. 2 shows the the set-up used for the measurement.

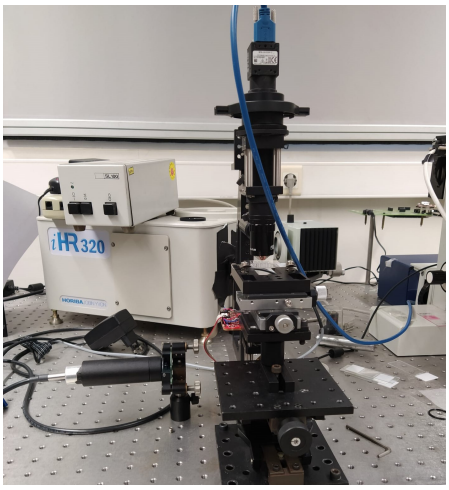

FIG. 2: A photo of the microscope without the sample on it.

III. BIREFRINGENCE DETERMINATION

Once the MM measurement has finished, an analysis program is used to determine some physical parameters that can be determined. From a MM measurement the program can determine Linear Dichroism (LD), Linear Birefringence (LB), Circular Dichroism (CD) and Circular Birefringence (CB). These effects are defined as:

$$LD = (k_x - k_y)\frac{2\pi d}{\lambda} \; ; \; LB = (n_x - n_y)\frac{2\pi d}{\lambda} \quad (10)$$

$$LD' = (k_{45} - k_{-45})\frac{2\pi d}{\lambda} \; ; \; LB' = (n_{45} - n_{-45})\frac{2\pi d}{\lambda} \quad (11)$$

$$CD = (k_L - k_R)\frac{2\pi d}{\lambda} \; ; \; CB = (n_L - n_R)\frac{2\pi d}{\lambda} \quad (12)$$

where n is the refractive index, k is the absorption coefficient and the subscripts indicate the direction of polarization.

With these characteristic values, it can be determined the value of the total linear birefringence(LB_m):

$$LB_m = (n_e - n_o)\frac{2\pi d}{\lambda} = \sqrt{LB^2 + LB'^2} \quad (13)$$

We can also understand LB and LB' as projections of the total birefringence

$$LB = LB_m \cos(2\alpha) \ ; \ LB' = LB_m \sin(2\alpha) \tag{14}$$

where α is the orientation of birefringence (the direction of the fast axis):

$$\alpha = \frac{1}{2} \arctan\left(\frac{LB'}{LB}\right) \tag{15}$$

To calculate the parameters in (10), (11) and (12) two methods can be used: one is extracting them from the differential Mueller matrix by doing the logarithm of the Mueller matrix, following the method discussed in [5]. The other one is extracting them form the Jones matrix calculated from the experimental MM. I will explain this last one since is the one used in these experiments, but both of them lead to the same results. First, the Jones matrix (2x2) must be found from the measured Mueller matrix. This calculus is rather involved and is well described in [4] (see these equations in section (14b) from the cited document). Once the measured Jones matrix is known, it can be compared with the general form of a Jones matrix [6] in order to obtain the polarization properties explained at the beginning of this section:

$$J = \begin{pmatrix} \cos\frac{T}{2} - \frac{iL}{T}\sin\frac{T}{2} & \frac{(C-iL')}{T}\sin\frac{T}{2} \\ -\frac{(C+iL')}{T}\sin\frac{T}{2} & \cos\frac{T}{2} + \frac{iL}{T}\sin\frac{T}{2} \end{pmatrix} \tag{16}$$

where

$$L' = LB' - iLD' \ \ ; \ \ C = CB - iCD \tag{17}$$

$$L = LB - iLD \ \ ; \ \ T = \sqrt{L'^2 + C^2 + L^2} \tag{18}$$

The details for the application of the previous equations are explained in [6]. In this work we will focus on the study of the parameters LB_m and α that are the most relevant ones to study the birefringence of starch granules. These parameters are calculated for each pixel and they are represented by the program in two separate and independent images. From the values of birefringence it is possible to evaluate the kind of structure (for example amorphous or crystalline) in the sample. For starch, when LB_m is represented, it can be seen that is homogeneous everywhere except for the center, and that for α it can be seen that it variates with the angle but not with the radius.

IV. STARCH GRANULES COMPOSITION

Starch is the main structure for storing energy in plants, and can be found in chloroplast as transitory starch granules and in amyloplast as reserve starch granules. It is found in roots, tubers and seeds. These granules are formed by two polysaccharides , one being amylopectin which makes between 70 to 85 percent of the granules and the other one being amylose which makes the rest [7]. These concentrations may differ in genetically modified starches.

Starch is formed in a concentrical way as it is shown in FIG. 3, starting at the hilum (center), and alternating amorphous lamellae made from amylose and crystalline lamealle made from amylopectin, giving as a result some darks areas in the study of birefringence corresponding to the amorphous medium.

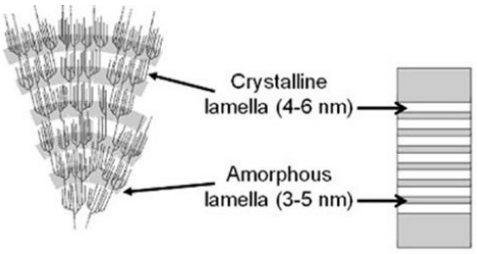

FIG. 3: Representation of the starch structure with the widths of each concentric layer and how are the polysaccharides disposed. Scheme from Ref. [8].

The amylose branches within the amorphous regions are produced less often and are smaller than the amylopectin branches which run through the structure of the starch an give it the crystalline properties.

V. MEASUREMENTS

All the measurements have been obtained by either using a microscope objective with x10 magnification or one with x50 magnification. This is important because the starch granules from sweet potatoes were very small and we needed the extra magnification with respect to the ones from the normal potatoes. In FIG. 4 an example of a measured MM for potato starch granules is provided. Note that a normalized MM scales between -1 and 1 as it is shown in color side bar. From the scale bar of the plot we can see the starch granules are around no larger than 25 μm in diameter.

When looking at the LB and LB' (shown in FIG.5) we can see a pattern that looks like a Maltese cross with four differentiated parts, two of them which are diagonal with a positive sign and the other ones with negative sign, meaning that the structure has a radial type of symmetry. Note that if there are small crystals in a circular disposition with variations in the direction of their axis, as $LB{=}LB_m \cos(2\alpha)$, LB will be zero for values of α corresponding to 0, 90, 180 and 270 degrees which corresponds with the results. Here the 0° angle is defined according to a certain arbitrary direction that has a relation with how the sample has been positioned on the microscope subjection structure.

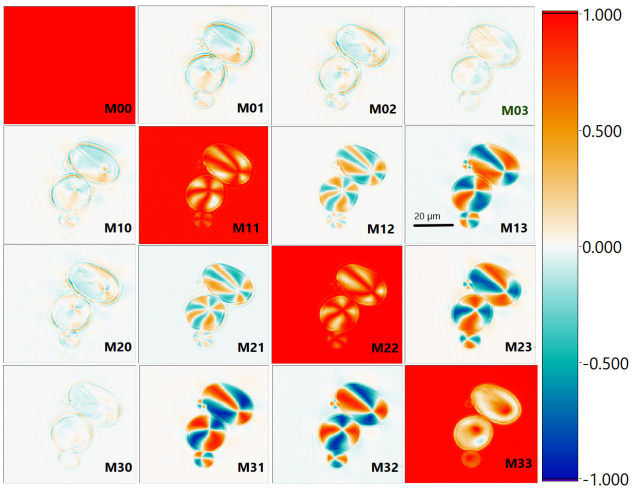

FIG. 4: Representation of the Mueller matrix for a group of starch granules from a potato.

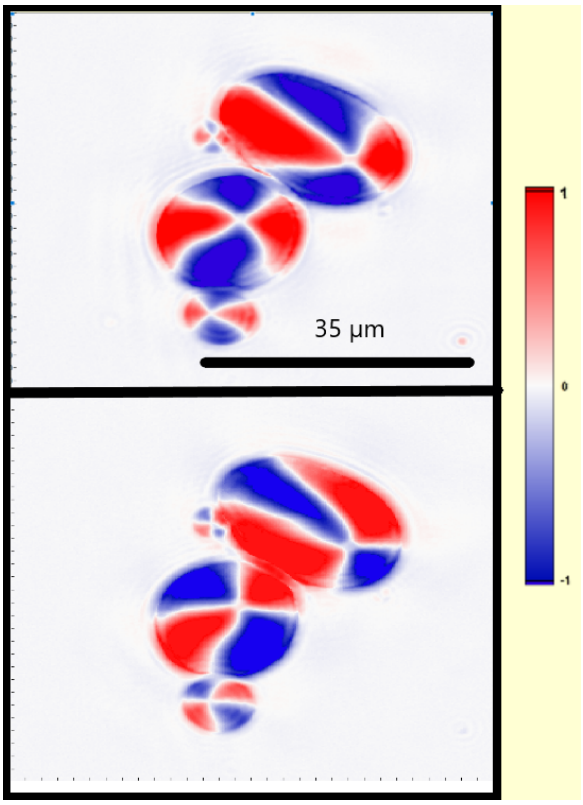

FIG. 5: Representation of the LB and LB' of the starch granules from a sweet potato.

FIG.6 shows that the total birefrigence stays almost constant through the granule except in the hilum due to the hilum being made of amorphous amylose [9]. We see that the total birefringence stays approximately constant thorough the whole area of the grain despite there are obvious changes in thickness due to the spherical shape. This is maybe caused by the inclination each crystal has inside the spherical grain: only the crystals in a central layer are perpendicular to the direction of light propagation and contribute to the measured retardation. As the angle between the light beam direction and the birefringent crystalline lamella becomes smaller, their overall contribution is lower. This phenomenon makes the central layer the only relevant layer in the birefringence measurement and the optical path travelled by the light outside this layer becomes mostly negligible in terms of birefringence effects.

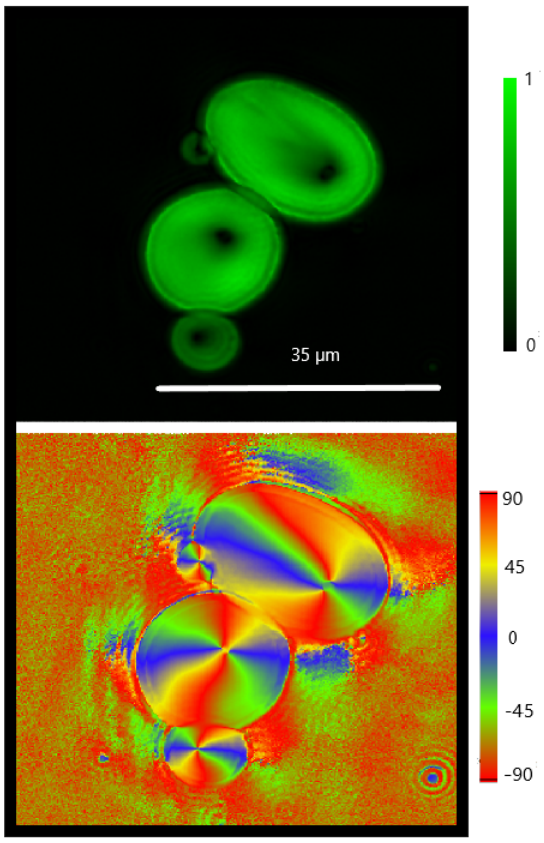

FIG. 6: Representation of the total birefringence and α of the starch granules from a potato.

The bottom panel of FIG. 6 also shows the angle α for the starch granule of a potato. Looking to this figure, it can be seen that the value variates if we rotate from a position with the hilum as the center, meaning that the crystal branches formed by the crystalline lamella were made in a radial way.

In FIG. 7 we can see the total birefringence of a starch granule of a sweet potato. Similar as in the case of the potato, we can see that it also has an amorphous hilum with zero total birefringence and a constant value of LB_m for the rest of the granule indicating a similarity with the one of a normal potato. The bottom panel of FIG. 7 shows the angle α for this sweet potato starch granule and it can be seen that it also has a radial structure.

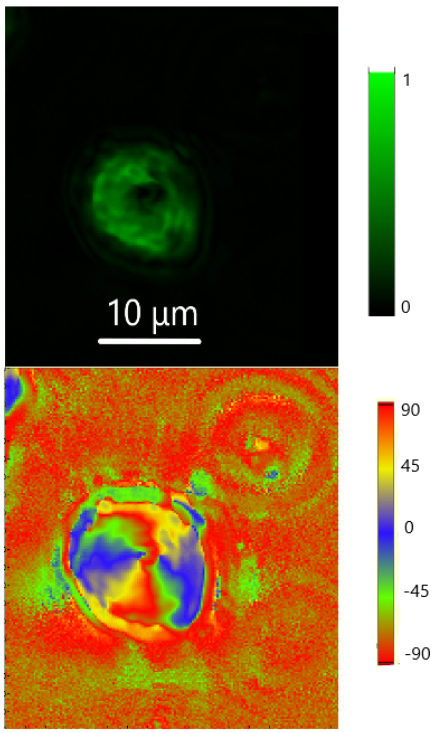

FIG. 7: Representation of the total birefringence and α of a starch granule from a sweet potato.

VI. CONCLUSIONS

- The studied starch granules are almost transparent and non depolarizing for 535 nm allowing a full study of the Mueller matrix without requiring extra material like a camera that measures circular polarization to obtain the last row of the MM.
- The starch granules differ in size for both tubers but they are formed with the same kind of radial microscopic structure and present very similar results when measuring the different values for the birefringence.
- The microscope has enough resolution to resolve small starch grains that are only a few microns in diameter. The microscope does not have enough resolution to distinguish the concentric amorphous rings within the grains.

Acknowledgments

I would like to thank Oriol Arteaga for all the support and help that has given to me during the all the process of making the TFG via online comunication, direct comunication and the amount of hours spent in the laboratory helping me. Without him this project could not have be done.

[1] A. Mendoza-Galván, Y. Li, X. Yang, R. Magnusson, K. Järrendahl, L.Berglund, H. Arwin. Transmission Mueller-matrix characterization of transparent ramie films; Journal of Vacuum Science and Technology B 38, 014008 (2020).

[2] Url from where the picture was extracted: https://www.framos.com/en/news/case-study-4d-technology-micro-polarizer-technology-makes-impossible-measurements-possible.

[3] R. Ossikovski, O. Arteaga. Completing an experimental nondepolarizing Mueller matrix whose column or row is missing.Journal of Vacuum Science and Technology B 37, 052905 (2019)

[4] R. Espinosa-Luna, D. Rodríguez-Carrerab, E. Bernabeua, S. Hinojosa-Ruíz. Transformation matrices for the Mueller–Jones formalism. Optik, 119 (16), 757-765 (2008).

[5] Url from where the mentioned method was described http://www.mmpolarimetry.com/circular-dichroism/

[6] O. Arteaga, A. Canillas. Pseudopolar decomposition of the Jones and Mueller–Jones exponential polarization matrices. J. Opt. Soc. Am. A.26. No.4(2009).

[7] E. Bertoft. Understanding Starch Structure: Recent Progress. Agronomy 7(3):56 (2017).

[8] E. O'Neill, R. Field. Underpinning starch biology with in vitro studies on carbohydrate-active enzymes and biosynthetic glycomaterials.Front. Bioeng. Biotechnol. 3, 136 (2015).

[9] Cai C, Zhao L, Huang J, Chen Y, Wei C. Morphology, structure and gelatinization properties of heterogeneous starch granules from high-amylose maize. Carbohydr Polym.102:606-14 (2014).